IIETA International Information and Engineering Technology Association
Advancing the World of Information and Engineering

Mathematical Modelling of Engineering Problems
Vol. 11, No. 6, June, 2024, pp. 1452-1462
Journal homepage: http://iieta.org/journals/mmep

Deflection Prediction of an Anti-vibration Mount by Finite Element Analysis

Baban K. Suryatal[1], Prashant K. Ambadekar[2], Jagannath S. Gawande[3], Kuldeep A. Mahajan[4], Vijaykumar K. Javanjal[5], Mahesh M. Sonekar[5], Rahul N. Yerrawar[4], Shravan H. Gawande[4*]

[1] Department of Mechanical Engineering, PDEA's College Engineering, Manjari (Bk), Pune 412307, India
[2] Department of Mechanical Engineering, SIES Graduate School of Technology, Mumbai 400706, India
[3] Department of Mechanical Engineering, P.E.S. Modern College of Engineering, S.P. Pune University, Pune 411005, India
[4] Department of Mechanical Engineering, M.E.S. College of Engineering, S. P. Pune University, Pune 411001, India
[5] Department of Mechanical Engineering, Dr. D. Y. Patil Institute of Technology Pimpri Pune, Pune 411018, India

Corresponding Author Email: shgawande@mescoepune.org

https://doi.org/10.18280/mmep.110606

Received: 22 December 2023
Revised: 18 February 2024
Accepted: 1 March 2024
Available online: 22 June 2024

Keywords:
chloroprene rubber, finite element analysis, anti-vibration mount, rubber deflection prediction

ABSTRACT

To ensure the safety and dependability of rubber components, deflection analysis and prediction play a crucial role in process of design. Material property testing and finite element analysis (FEA) are combined to forecast the maximum deflection of a railway elastomeric pad. IRMRA (Indian Rubber Manufacturer's Research Association) developed the chloroprene rubber. Using the FEA method, maximum deflections of an anti-vibration mount under several compressive loads are calculated. Mooney-Rivlin nonlinear hyperelastic three parameter model with element type Plane 182 is used for and FEA. Curve fitting of the uniaxial tensile test results is used to extract three parameter Mooney-Rivlin model constants by using FEA. Then, these Mooney-Rivlin model constants are used to analyze anti-vibration mount and predict the deflections at different compressive loads. The outcomes are contrasted with the technical specifications provided by the Research Designs and Standards Organization of Indian Railway and predicted deflections are within the limits of maximum values allowed. The results are also contrasted with data from literature, and 10% variation is observed between results obtained and literature results. This methodology can be used to predict deflections of any newly developed rubber at initial stage of design.

1. INTRODUCTION

Due to their vast elastic reversible deformation, absorption of energy, and superior damping properties, rubbers are commonly used in a variety of applications. Standard uses contain mounts for engine and automobile tires, electric appliances for household, bridge rubber bearings, and vibration isolators for railroad wagons. The majority of these rubber parts are loaded both statically and dynamically while in use. One of the most important considerations in rubber parts design is operational problems prevention [1]. To ensure the security and dependability of mechanical rubber components, analysis of deflection and strength estimation are crucial steps in the process of design. Bench compressive tests, road simulation tests, and real road tests have been the main methods used to evaluate the compressive strength of rubber components [2]. The compressive strength test should always be performed anytime a material or geometric modification is made, even though these approaches have advantages in terms of accurate compressive strength estimation. Therefore, the rubber parts design requires estimation of compressive strength which will be obtained by tests of specimen and analysis of parts [3]. In this study, a methodology is established to forecast the deflections of railway anti-vibration mount under various loads with the help of tests of material property and FEA modeling. The objective of this work is to predict the deflection of an anti-vibration mount at different compressive loads before manufacturing the actual rubber mount which will helpful at early design stage. If the deflections of the mount are within the permissible limits, then only the life and working of mounts will be satisfactory. On the investigation and material characterization of rubber, there is a wide body of literature. The section that follows discusses some of the work.

Yeoh [4] addressed the unique characteristics of the rubber Ogden strain-energy function material model, which is starting to gain traction among finite element analysis users. It illustrates why an Ogden strain-energy function produced by nonlinear regression analysis of stress-strain data derived from just one mode of deformation may be unsuitable for forecasting behavior in other deformation modes. It advises that some of the coefficients in the regression analysis be chosen in accordance with the behavior of rubbery materials. A rubber mount's fatigue life was predicted by Li et al. [5] by integrating FEA and property tests of material. Uniaxial tensile test and fatigue life tests of natural rubber were used for obtaining fatigue life equation of materials like natural rubber. In order to anticipate the rubber mount's fatigue life, total

maximum primary strain was employed as parameter of fatigue and replaced into fatigue life equation of rubber. Then, for verifying precision of the prediction approach of fatigue life, rubber mount's fatigue lives under various loading conditions were tested using test rig. The rubber fatigue behavior is examined by Ali et al. [6] utilizing dumbbell specimens subjected to uniaxial strain. A damage model (continuum) created on the function of strain range under loading in cyclic nature is proposed for modeling fatigue damage behavior. The constitutive relationship of natural rubber is defined in terms of the Ogden strain energy potential. The effects of formulation of rubber, history of loading in mechanical conditions, environmental parameters and rubber's constitutive response in dissipative aspects were reviewed by Mars and Fatemi [7] as the four main groups of factors that affect the life of rubber parts in mechanical fatigue. Primary criteria are explained for each category, and available literature is given and reviewed. Boyce and Arruda [8] explore models (constitutive) for rubbery material's response under restricted deformation. Discussion and comparison of various statistical and continuum mechanics of rubber elasticity incompressible models with experimental data are presented. Taking into account the impacts of the mean load, Kim et al. [9] calculated an engine mount's life in fatigue composed of rubber (natural). Using dumbbell specimens with three dimensions at various mean loads, load controlled fatigue tests were carried out to define suitable damage criterion (fatigue) for material like rubber. Green-Lagrange strain (maximum) and natural rubber equation of fatigue life curve were used to estimate life of rubber engine mount under fatigue loading.

The application of an energetics method to address several facets of rupture and fatigue in elastomers was addressed by Lake [10]. Included in the discussion are cavitation, friction, abrasion, adhesion, (under conditions where same is primarily influenced by contact breaking and making), tearing, fatigue and crack growth, failure in tension, effects due to oxidation, cracking due to environmental conditions, and sharp objects cutting. As well as discussing the material properties tying different types of cohesive failure together, physical and chemical aspects determining fracture growth characteristics are also covered. The use of FEA in design of product at several development steps, from characterization of material rupture to forecasting performance of design at end, was discussed by Morman and Pan [11]. Oh [12] used the energy balance concept—that is, the energy available verses the energy needed to extend a tear—to establish model for the rubber bushing's life in fatigue. This model and the test results correlated well. From the model, a design process was created that provides the ideal insert shape for the longest possible bushing life. In order to study how the hysteresis energy loss and input energy depended on the repeated strain, the quantity of deformations, the rate of extension, and temperature, Hirakawa et al. [13] evaluated the hysteresis energy loss and input energy directly in the dynamic state. They then correlated these to the fatigue life.

Mullins [14] noted that rubber softens as a result of deformation, and that first curve of stress-strain established during first elongation is distinct as well as immutable. Repeated deformation also has the effect of bringing the stress-strain curve of rubber asymptotically closer to equilibrium or a steady state. A detailed comparison of twenty models for hyper-elastic rubber materials is presented by Verron and Marckmann [15]. Analysis is done on these models' capacity to replicate various loading circumstances. For 25% modest strokes of oscillation, Cadwell et al. [16] illustrated of the curve of fatigue life (dynamic) showed its common characteristics. Rubber is found to have a minimum dynamic fatigue life under linear vibrations when return stroke returns sample to state of no strain. Saintier et al. [17] studied onset of fatigue flaws in a natural rubber under multi-axial non-proportional loadings. Results of tests involving torsion, push-pull, and compression-tension with fatigue in static torsion overlay are provided. Under relaxing loading circumstances, Le Cam et al. [18] examined development of fatigue flaws in a cis-1, 4-polyisoprene rubber packed with carbon black. The determination of the fracture growth scenario is the study's main objective. According to Lindley [19], energy in minimum quantity is required for propagation of fractures by the process of tearing under deformations of cyclic nature in which rubber (natural) is permitted to fully relax is around 0.04kN/m, and in that case, hysteresis is not involved. According to Mars and Fatemi [20], rubber parts exposed to varying loads frequently fail as a result of propagation and initiation of flaws. Understanding mechanics behind failure process is necessary for prevention of similar failures. Presently available analysis methods for forecasting rubber life are reviewed in this research.

According to Saintier et al. [21], the increasing usage of elastomers and polymers in constructions necessitates the development of appropriate multi-axial fatigue life standards for these materials. Therefore, it is crucial to comprehend the micro-mechanics of fatigue fracture initiation and how they relate to the history of local stress and/or strain. These natural rubber micro-mechanics have been studied with the help of SEM (scanning electron microscopy) and EDS (energy dispersive spectroscopy). The crack initiation was consistently accompanied by rigid inclusions. The initial damaging processes seen are cavitation at the poles or decohesion, depending on the type of inclusions (detected by EDS). The orientations of the cracks are compared with the history of the local principal stress orientation, which is derived from finite element computations (FE). It is demonstrated that even under non-proportional loading, cracks are observed to propagate systematically in the direction indicated by the maximal first primary stress reached during a cycle if big strain circumstances are appropriately taken into account. With the aim of evaluating impacts of carbon black on fatigue life, J-value (critical), surface morphology of fracture, and hysteresis, Kim and Jeong [22] experimentally investigated the rubber compounds (natural) filled with N990, N330 or N650. It was observed that square root of product of hysteresis and J-value (critical) and fatigue life logarithmic value were linearly proportional. A study by Mars and Fatemi [23] examines methods such as maximum main strain (or stretch), criteria of octahedral shear strain and density of strain energy that are frequently used for rubber fatigue crack nucleation investigation. The capacity to anticipate multi-axial fatigue behavior using these old equivalent criteria and a more contemporary equivalence criterion based on cracking energy density are also investigated. The theoretical underpinnings of the application of various fatigue life analysis methodologies are also introduced. Multiaxial fatigue life prediction of elastomers was carried out by crack initiation damage criteria. This method was validated by performing the experiments with different loading conditions and amplitudes under out of phase and in – phase torsion – axial tests. Based on the maximal normal strain plane and damage quantification by cracking energy density on that plane, a critical plane approach

was determined to be the most effective way for crack initiation life prediction for complicated multiaxial variable amplitude loading. To forecast fatigue life under varying amplitude loadings, Miner's linear damage rule and the rainflow cycle counting approach were applied. The component's overall fatigue life was predicted using the fracture mechanics approach using specimen crack growth data and FE simulation results.

Elastomeric matrix composites, according to Legorju-jago and Bathias [24], are frequently reinforced with mineral particles like carbon black and occasionally with fibers of organic or long metallic. Rubbers are capable to categorize as nanocomposites in fiber absence. Elastomers are damaged by cyclic loading to the point that one or more cracks occur and spread. Compression loading is crucial because chemical transformations like crystallization have an impact on fatigue resistance. To extend the fatigue life of rubber springs, Luo and Wu [25] performed FEA analysis. It is demonstrated that utilizing nonlinear software, simulation (quasi-static) of springs made of rubber can offer useful insights into analysis of failure and design of product. It is demonstrated that component's profile of fatigue (virtual), which offers a clear picture of prospective failures, can be retrieved utilizing user subroutines and post-processor. Under uniaxial conditions of loading, Le Cam et al. [26] investigated macroscopic level fatigue damage in natural rubber filled with carbon black. Until the samples failed, conditions of uniaxial tension loading (non-relaxing and fully relaxing), and compression- tension were used. For uniaxial compression- tension and tension loading (uniaxial) under full relaxation circumstances, one form of damage due to fatigue is seen, however numerous other types of damage due to fatigue are seen in tension loading (uniaxial) under non-relaxation conditions. Various types of impairment that can be seen when rubber is subjected to tension loading (uniaxial non-relaxing) are strongly interrelated to extension of fatigue life. According to Verron and Andriyana [27], from an engineering perspective, predicting the onset of fatigue cracks in automobile rubber parts is a crucial step before designing new parts. They have developed a brand-new predictor for rubber fatigue fracture nucleation. It was created within the context of configurational mechanics and is inspired by microscopic mechanisms brought on by fatigue. Results indicate that the current predictor, which incorporates the predictors that have already been published, is able to combine data on multi-axial fatigue.

For rubber-like materials that have undergone significant elastic deformation, Ali et al. [28] examined the requirements of various constitutive models. The constitutive models are frequently employed in rubber component Finite Element Analysis (FEA) software programs. This evaluation gave engineers and manufacturers a solid foundation for making decisions about which constitutive model to use for incompressible and isotropic materials out of a variety depending on strain energy potential. Mars and Fatemi [29] conducted experiments utilizing cylindrical short specimens with thin-walled exposed to twist and axial displacements to examine impact of multi-axial stress on fatigue fracture formation and progress in rubber (filled natural). Correlations between the peak maximum primary strain and fracture nucleation lifetimes and growth rates were discovered and are explored. The peak maximum primary strain is the largest lateral or longitudinal strain depending upon the loading direction. These correlations are significant because in comparison to the monotonic response, the cyclic stress-strain response shows a substantial early softening, followed by a more gradual additional softening. The first softening is thought to be caused by irreversible breakdown of different kinds of bonds, and the second softening is thought to be caused by fillers and their impact on network chain breakage. According to Woo and Kim [30], fatigue study and lifespan evaluation are crucial steps in process of design to guarantee security as well as dependability of parts made by rubber. By combining results of FEA with damage parameter of fatigue obtained from the test of fatigue, an approach for predicting life of vulcanized natural rubber was developed. The damage parameter of fatigue is calculated using Green-Lagrange strain at the crucial region identified by the finite element approach. According to Andriyana and Verron [31], continua cannot be entirely regarded as defect-less. During experimental interpretations, it was discovered that natural rubber has dispersed tiny flaws that amplify under cyclic loading. These findings, however, are not taken into account by the traditional rubber fatigue life predictions, namely strain energy, maximum principle stress and stretch. Inelastic constitutive equations are added to a predictor based on configurational mechanics. Then, it is applied for forecasting fatigue life. According to Stevenson et al. [32], integrating fatigue life estimations into the design process is a significant difficulty in design with rubber parts for automobile applications such as mounts for engine and suspension mounts for chassis. They outline the process for calculating the fatigue life of elastomeric parts and use a rubber bearing case study that was distorted by compression and shear bi-axial combination to demonstrate their points.

Thus, by going through the literature survey of analysis of rubber like materials it is concluded that continuum-based mechanical models can explain materials that resemble rubber. The field of accurate constitutive modelling has yielded multiple models that describe the elastic energy in relation to the deformation. The models are based on stretch ratios or strain invariants. Many applications benefit greatly from the use of traditional hyperelastic material models, such as the Mooney-Rivlin or Ogden models. Theoretically, Ogden and the Mooney-Rivlin polynomial have identical outcomes. Regarding their formula, the approaches differ from one another, nonetheless. The strain energy density of the Mooney-Rivlin model is based on the principal strain invariants, while the Ogden model provides the strain energy density based on three principal stretches. In general, the number of parameters, the kind of formulation used to construct the models, and the domain of validity for all kinds of deformation are used to classify the models. Thus, depending on the area of deformation under consideration, the following models can be applied: for small, moderate, and large strain, respectively: the neo-Hookean model, the Mooney model, and the Ogden model. It is found that the different researcher uses a variety of mathematical models to predict the life or failure. There were a very few research groups which were used deflection due to compressive load as a life prediction criterion. In this work, the railway wagon anti-vibration pads are subjected to a heavy compressive load, therefore, deflection due to these loads is predicted using FEA and material test properties which is used as basis for life prediction or failure of the rubber pads.

2. SHOCK AND VIBRATION ISOLATION PRINCIPLE

A motion in which there is a sharp, unexpected shift in velocity is referred to as a shock. Shock typically involves a single, intense energy impulse with a rapid acceleration. Shock isolation limits the forces that are communicated to the area around the equipment from which the shock originates. The usage of isolators, which results in the storage of the shock energy within the isolator and its release of energy over a lengthy period of time, allows for the decrease of shock. The isolator's deflection allows for the storage of energy. Instead of transmissibility (like with vibration isolators), the efficiency of a shock isolator is determined by the transmitted force and the resulting deflection. Vibration is a magnitude (force, displacement, or acceleration) that oscillates about a mean reference. Shocks must be dampened, whereas vibrations can be isolated, hence the two are dealt with differently. Designing an appropriate compound and preserving modulus at a level that will satisfy the load-deflection requirement of a certain design is the responsibility of the rubber technologist. Natural rubber will be the best elastomer if damping is not present because it can be compounded to keep its ideal elastic properties over an extended length of service [31]. The goal of isolation is to reduce the amount of vibrational disturbance that is transmitted from the source to the receiver.

Because of their unfeasible high frequency ratio, rubber mounts are typically ineffective for very low frequency applications. In these cases, the natural frequency of the isolator must be lowered, either by altering its mass (since it is inversely proportional to natural frequency) or its stiffness. Since altering the mass of the isolator is often impractical, one must alter the other directly proportional quantity (i.e., the stiffness), such as by adding fillers or cork powder (which coincidentally also improves damping by hysteresis), or by using reinforcing wires or inserts. Such situations always call for a unique design. For vibration isolation, an elastic composition is advised; nevertheless, in particular applications, additional dampening is desired to reduce resonance increase or hasten die-out in the event of shock. The key terms of the shock and vibration isolation principle are defined as below:

Vibration: It can be defined as a force, displacement, or acceleration whose magnitude oscillates around a given reference point, alternating between being smaller and greater than the reference. Frequency in cycles per second, or Hz and amplitude which is the magnitude of the force, displacement, or acceleration, are two terms to describe vibration.

Frequency: The quantity of full oscillation cycles that take place in a certain amount of time is known as frequency.

Period: The amount of time needed for a single vibration cycle.

Forcing Frequency: The number of oscillations per unit of time caused by an external force or movement applied to a system is known as the forcing frequency.

The number of oscillations a system will undergo in a unit of time if it is moved from its equilibrium position and permitted to vibrate freely is known as its natural frequency.

Amplitude: The zero to peak value that corresponds to the maximum magnitude of a harmonic vibration time-history is the amplitude of a harmonic vibration, such as displacement, velocity, or acceleration.

Spring stiffness is defined as the ratio of a force increment to a corresponding spring deflection increment.

Damping: In a vibratory system, damping is the process through which energy is lost. There are three types of damping that are commonly used: viscous, coulomb, and hysteresis.

Coulomb Damping: A vibratory system is said to have coulomb, or dry friction damping if the damping force in the system is constant and unaffected by changes in position or velocity.

Hysteresis (Inherent) Damping: Hysteresis damping is the type of damping that happens when a material is subjected to motion and is caused by the molecular structure of that substance. Good examples of materials with this kind of damping are elastomers.

Viscous Damping: Any particle in a vibrating body is said to be viscously damped if it experiences a force that is proportionate to its velocity in a direction that is opposed to its velocity.

Critical Damping: When a system is moved from its initial static position and most quickly returns to it without experiencing any over-oscillation, it is said to be critically damped.

Resonance: A suspension system is said to be in resonance when the forcing frequency and natural frequency of the system coincide.

The ratio of the dynamic output to the dynamic input is known as transmissibility.

2.1 Vibration isolation without damping

There are three components involved in the transmission of vibration: A source that produces an excitation force or displacement, a conduit that the vibratory disturbance travels through, and a receiver. Reducing the amount of vibrational disturbance that is transferred from the source to the recipient is the aim of isolation. Fundamental to comprehending vibration isolation is the one degree of freedom model, which describes the uniaxial behavior of a linear system composed of a lumped mass and spring and damping elements [3]. Figure 1 depicts the model for the undamped situation.

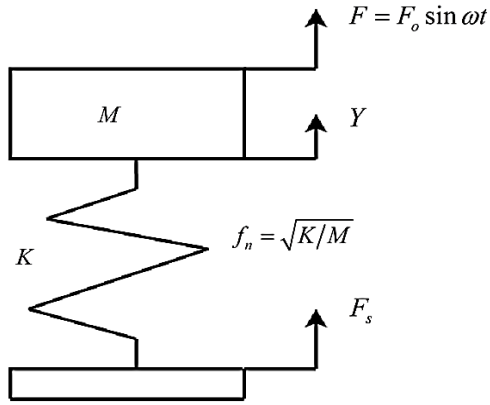

Figure 1. Undamped single degree of freedom model [3]

When a mass, *M*, experience a sinusoidal excitation force, *F*, in a steady state, the displacement of the mass is:

$$Y = \frac{F_0/M}{\left(\frac{K}{M}\right) - \omega^2} \sin \omega t \tag{1}$$

The system's natural frequency (measured in radians per second) is given as follows:

$$f_n = \sqrt{K/M} \tag{2}$$

By dividing the numerator and denominator of Eq. (2) by K/M and replacing for f_n, the displacement of the lumped mass is expressed as follows:

$$Y = \frac{F_o/K}{1-\left(\omega^2/f_n^2\right)}\sin\omega t \tag{3}$$

The dynamic displacement is a function of the static deflection divided by the ratio between the frequency of the sinusoidal excitation force and the natural frequency of the system, according to an analysis of the numerator and denominator in Eq. (3). The isolation system's objective is to lower the force communicated to the support to a level that is less than the excitation force acting on the mass. The force exerted on the support is stated by using Eq. (4) as follows:

$$F_s = (K)(Y) \tag{4}$$

The ratio of the force acting on the mass to the force acting on the support is known as the transmissibility through the spring and is given by Eqs. (5) and (6) as below:

$$T = \frac{F_s}{F} = \frac{(K)(Y)}{F_o \sin\omega t} \tag{5}$$

$$T = \frac{1}{1-\left(\omega^2/f_n^2\right)} \tag{6}$$

Figure 2 provides a graphic representation of the magnitude of Eq. (6). A closer look into Eq. (6) reveals some significant aspects of the behavior of the undamped system. When $\omega/f_n=1$, there is infinite transmission. As the excitation frequency rises, the transmitted force decreases until it equals the excitation force when $\frac{\omega}{f_n} = \sqrt{2}$, at which point the transmissibility is unity. A positive value of transmissibility comes from Eq. (6) as well when $\omega<f_n$, indicating that the force acting on the support is in phase with the excitation force. If the reaction force is out of phase with the excitation when $\omega>f_n$, the transmissibility value will be negative.

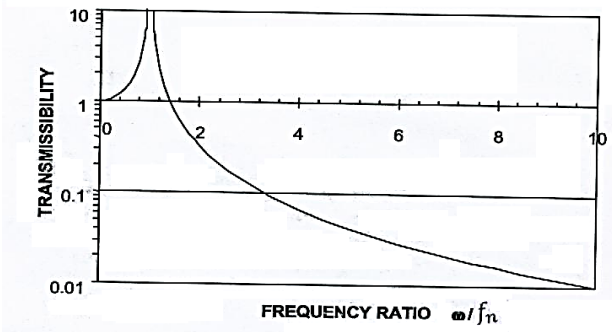

Figure 2. Undamped system transmissibility [3]

The natural frequency of the system depends on the static deflection of the isolator caused by the weight of the attached body if the isolator displays a linear force vs. deflection curve. Transmissibility can therefore be represented as a function of the static deflection of the isolator because transmissibility is a function of the system's natural frequency and given by Eq. (10) as below:

$$f_{n1} = \frac{f_n}{2\pi}\sqrt{(K)(1000)/M} \tag{7}$$

$$f_{n1} = 5.0329\sqrt{K/M} \tag{8}$$

$$f_{n1} = 15.76\sqrt{1/\Delta_s} \tag{9}$$

$$T = \frac{1}{1-\left(4\pi^2/9804\right) f^2 \Delta_s} \tag{10}$$

where, M= mass of the mounted body in Kg; K= stiffness of the isolator in N/mm; f_{n1}= natural frequency of the system in Hz; f= frequency of force excitation; Δ_s= static deflection of the isolator in *mm*. Eq. (10) defines the relationship between transmissibility and static deflection which is represented graphically by Figure 3. This graph is significant because it shows how much static deflection an isolator needs to have in order to achieve a particular level of isolation.

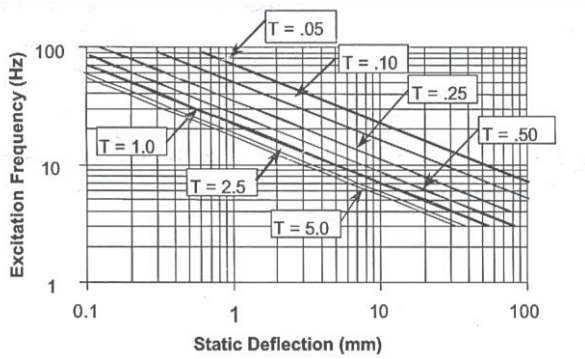

Figure 3. Transmissibility as a function of static deflection and excitation frequency [3]

2.2 Vibration isolation with viscous damping

The following Figure 4 depicts the single-degree-of-freedom model with viscous damping.

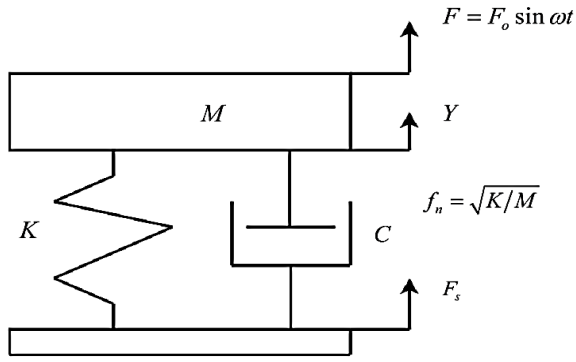

Figure 4. Viscous damping model [3]

The following Eq. (11) represents transmissibility for the damped condition:

$$T = \frac{\left(K^2+\omega^2C^2\right)^{1/2}}{\left[\left(K-m\omega^2\right)^2+\omega^2C^2\right]^{1/2}} \tag{11}$$

Eq. (11) can be generalized to the situation when damping and stiffness are both frequency-dependent as follows:

$$K_\omega = \text{Stiffness at frequency } (\omega)$$

$$C_\omega = \text{Damping at frequency } (\omega)$$

$$\delta_\omega^2 = \frac{\omega^2 C_\omega^2}{K_\omega^2}$$

f_n = Natural frequency of the system

$f_n^2 = \frac{K_o}{M}$, where K_o = Stiffness at frequency f_n

$$T = \frac{\left(1+\delta\omega^2\right)^{1/2}}{\left\{\left[1-\left(\omega/f_n\right)^2\left(K_o/K_\omega\right)\right]^2+\delta_\omega^2\right\}^{1/2}} \tag{12}$$

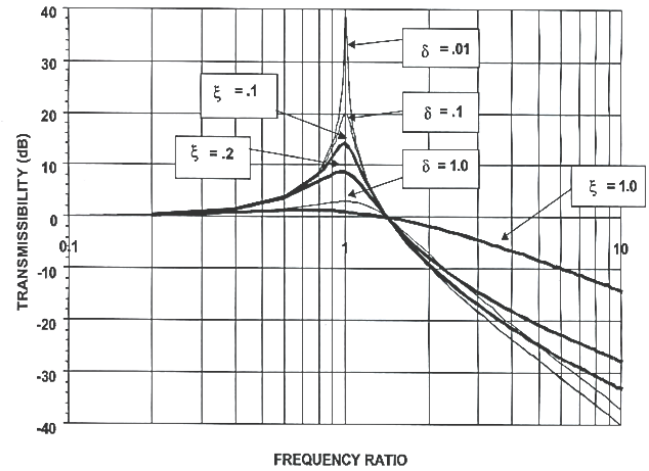

Figure 5. Transmissibility for a damped system [3]

Figure 5 depicts Eqs. (11) and (12) graphically. As can be seen by looking at the graph, the presence of damping in the system results in a higher level of transmissibility at frequencies higher than $f_n \times \sqrt{2}$, and reduces the amount of transmitted force at resonance. The force transmitted through the damping element is what causes the higher level of transmissibility above $f_n \times \sqrt{2}$. When evaluating Eq. (11), the magnitude of damping is stated in terms of ξ, this is the ratio to the critical damping C_c, and is described below [33]:

$$C_c = 2\sqrt{K_o M} \tag{13}$$

$$\xi = \frac{C}{C_c}$$

The value of transmissibility in Figure 5 is given in terms of a decibel (dB), as opposed to being expressed as an absolute value. Eq. (14) outlines the decibel's definition.

$$T_{dB} = 20\log\left(T/T_{\mathrm{Re}\,f}\right) \tag{14}$$

The basic way to achieve isolation is to keep the disturbing frequency's relationship to the system's natural frequency in check. The inherent frequency of the isolator, or more accurately, the inherent frequency of the system made up of the isolator and mounted equipment, is one of its features. Every degree of freedom in a system generally has a natural frequency; the single-degree-of-freedom system has a single natural frequency. As, C=C_c in case of a critical damped system, therefore, there is no natural frequency of oscillation and returns to equilibrium without oscillation if relocated.

An isolator's features are frequently defined using the idea of static deflection. The isolator's deflection under the stationary or deadweight force of the attached equipment is known as static deflection. Thus, it seems that monitoring the static deflection alone can yield the natural frequency of a single-degree-of-freedom system. With certain qualifications, this is accurate. First, there must be a straight line on the force vs. deflection graph for the spring to be considered linear. Second, the elasticity of the robust material needs to be the same in both static and dynamic settings. This latter condition is typically satisfied by metallic springs, although many organic materials utilized in isolators do not. These materials have a higher dynamic modulus of elasticity than static modulus; as a result, the natural frequency of the isolator is somewhat higher than that determined just by static deflection.

If the system will be in resonance and then the disturbance forces will be enhanced rather than decreased when it is excited at its natural frequency. It is therefore highly desirable to choose the appropriate isolator such that its natural frequency will not coincide with any equipment critical frequencies and will be excited as little as possible when in use. Most isolators have dampening of one kind or another. Because damping helps to limit transmissibility, it is useful when the mounted system is working at or near its native frequency. Take an internal combustion engine, for instance, that is supported by steel springs that don't provide much dampening. The engine's disturbing frequency will eventually match the spring-mass system's inherent frequency upon engine start-up and as engine RPM increases. Light damping will result in a very big build-up of forces from the engine to the support, which will increase transmissibility. Serious damage to the engine or support chassis may occur if the engines idle RPM falls within the range of the spring-mass system's inherent frequency. On the other side, resonance amplification would be significantly reduced if the designer chose an elastomeric isolator with a higher damping degree.

3. CHARACTERIZATION OF MATERIAL

3.1 Chloroprene rubber hyperelastic material modeling

First and foremost, a good anti-vibration material should have a high damping factor that does not significantly rise with frequency. It should also not have any significant frequency-dependent increases in its dynamic modulus. The different materials used for anti-vibration mounts are natural rubber or polyisoprene (NR), synthetic isoprene (IR), styrene-butadiene (SBR), butyl or polyisobutylene (IIR, CIIR), poly-urethane, silicon (VMQ), and neoprene (polychloroprene). Each material has their own advantages and disadvantages. Natural rubber is good at absorbing vibrations because of its high elasticity and dampening qualities. It isn't as resistant to heat, oil, and some chemicals, though, as some synthetic rubber varieties are. The chloroprene rubber falls under the category neoprene (polychloroprene). Chloroprene is a synthetic rubber with a broad temperature range of flexibility and strong chemical resilience. It may be used in tough locations because

it is resistant to chemicals and oil. Chloroprene rubber has moderate resistance to solvents, outstanding ageing properties and resistance to fire. It also addresses the wide range of NR and IR technical features as compared to other type of rubbers. Therefore, due to these advantages, the chloroprene rubber is selected for the railway wagon anti-vibration mount.

Figure 6. Photograph of an anti-vibration mount

A rubber material made of chloroprene is developed by IRMRA, Thane, for a railway elastomeric pad shown in Figure 6 as per the specified properties by Research Designs and Standards Organizations, Lucknow. An elastomeric pad's rubber material is rubber made of chloroprene in vulcanized form, with 66 Shore A hardness. The technical details of the above mentioned anti-vibration mounts are as below:

Material: Rubber pads – Chloroprene rubber, Steel plates-IS: 2062-Fe 410 WA (modulus of elasticity, $E = 2\times10^5$ N/mm^2, Poison's ratio, υ=0.3), Manufacturing Process–Injection molding process. Rubber material made of Chloroprene can be observed as hyperelastic behavior because of its incompressibility and extremely nonlinear elastic isotropic behavior. In case of hyperelastic material a correlation between stress and strain is commonly characterized by strain energy potentials, which is necessary for the FEA of rubber components [34]. To characterize the hyperelastic material behavior, or the constitutive relation, experimental test data are required to determine the material properties in the strain energy potential.

A constitutive model can be used to describe any material. This model represents the traditional link between strain and stress. While this approximation holds true for certain materials, stress is dependent on factors other than strain in other materials. This is the situation with materials that resemble rubber and have extremely intricate material behavior. The majority of engineered rubber-like materials show significant material damping in addition to their nonlinear elastic behavior, which causes a hysteretic reaction to cyclic loading. In addition to the strain level, the current strain rate and strain history also affect this dynamic reaction. When a harmonic load is applied to the material, for example, this behavior can be seen in the dependence on frequency and amplitude, respectively. These dependences can result in variations in the dynamic modulus and damping of common engineering rubber-like materials of several hundred percent. Mooney's theory, which was developed in 1940, was one of the early phonological theories that addressed major deformations. It was widely recognized and had a significant impact on the development of this subject. The foundation of Mooney's theory is the presumption that the Hook's law is followed in simple shear and that the elastomer is incompressible and isotropic in the undeformed shape. As most elastomers are thought to be almost incompressible, the first assumption accurately captures the reality. Regarding the second supposition, simple shear up to moderate deformations are rather adequately described by Hook's law. Rivlin expanded on the phonological technique to explain the hyperelastic behavior of materials that resemble rubber. Rivlin contended that the power series should be used to approximate the strain energy function for an isotropic material. In this study, constitutive model of the chloroprene rubber material is specified using Mooney-Rivlin function. Mooney-Rivlin model's strain energy potential can be stated as [35]:

$$W = \sum_{i+j+k=1}^{\infty} C_{ijk}(I_1-3)^i(I_2-3)^j(I_3-3)^k \tag{15}$$

where, set of constants C_{ijk} are calculated by material testing and first, second and third order invariants of strain I_1, I_2 and I_3 respectively are expressed as:

$$I_1 = \lambda_1^2 + \lambda_2^2 + \lambda_3^2 \tag{16}$$

$$I_2 = (\lambda_1\lambda_2)^2 + (\lambda_2\lambda_3)^2 + (\lambda_3\lambda_1)^2 \tag{17}$$

$$I_3 = (\lambda_1\lambda_2\lambda_3)^2 \tag{18}$$

Principal stretch ratios λ_1, λ_2, and λ_3 in uniaxial stress state, are represented as:

$$\lambda_1 = \lambda u, \lambda_2 = \lambda_3 = 1/\sqrt{\lambda_1} \tag{19}$$

The values (I_1-3), (I_2-3) and (I_3-3) are used instead of I_1, I_2 and I_3 to ensure, by convention, that the strain energy function has a value of zero in the unstrained condition. In a similar manner, the parameter C_{000} in the same state is assumed to be zero. The third invariant I_3 can be understood in physical terms as the square of the ratio between a material element's volumes in its deformed and undeformed states. Thus, it may be inferred that, with respect to incompressible materials, $\lambda_1\lambda_2\lambda_3$=1 and I_3=1.

In loading direction, principal stretch ratio is λ_u and stretch ratios (principal) along loading direction perpendicular planes are λ_2 and λ_3. In order to increase stability, Mooney-Rivlin model with three variables provided by Eq. (20) is chosen in this work to characterize the chloroprene rubber's constitutive model.

$$W = C_{10}(I_1-3) + C_{01}(I_2-3) + C_{11}(I_1-3)(I_2-3) \tag{20}$$

The strain energy density function of a material and its hyperelastic constants dictate the material's mechanical reaction. Therefore, it is essential to precisely evaluate the material constants of the materials under examination to achieve successful results during a hyperelastic study. Typically, experimental stress-strain data of the material under consideration is utilized to derive the material constants. It is advised that test data be collected throughout a broad range of strain values and from multiple modes of deformation. It has been noted that to attain stability, test data in at least as many deformation states as will be encountered during the analysis should be used to match the material constants. A basic deformation test (uniaxial tension) is typically employed for

hyperelastic materials to precisely characterize the material constants. ANSYS software is utilized to perform hyperelastic material curve fitting on the uniaxial tensile stress-strain data acquired during the test. This process determines the material constants in the nonlinear three-parameter Mooney-Rivlin model. The test data of rubber made of chloroprene under uniaxial tensile loading shown by graphical form in Figure 7 are used to calculate constants C_{10}, C_{01}, and C_{11}. Uniaxial tensile test's data fitting; we determined that C_{10}= 0.1414791, C_{01}=-0.1163389, and C_{11}=0.01248255.

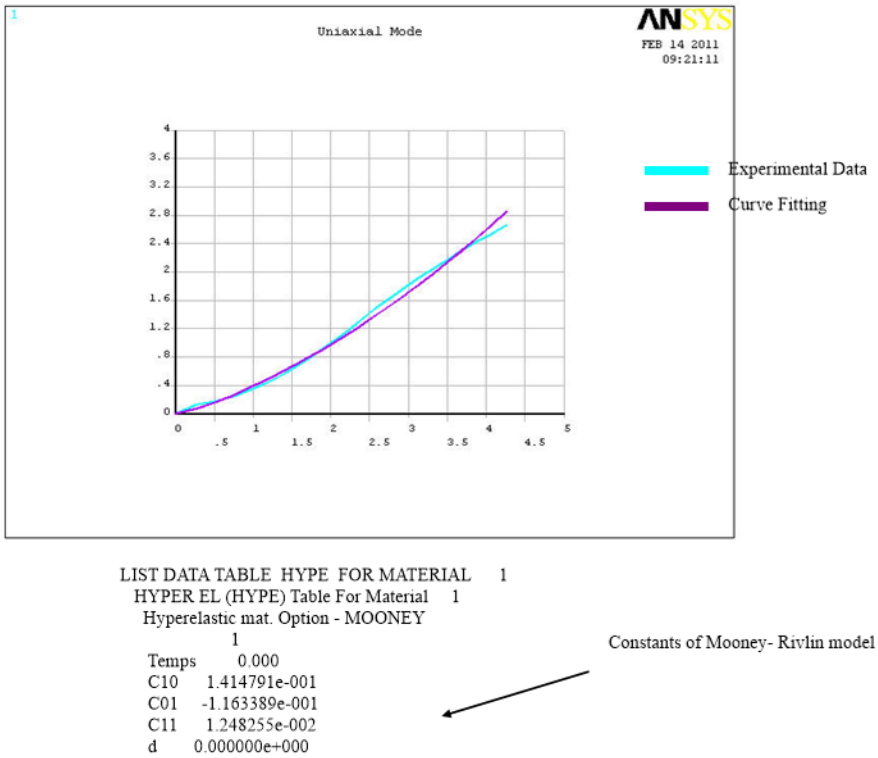

Figure 7. Developed rubber's stress-strain curves under uniaxial tensile load

3.2 Chloroprene rubber test of compression

A test is carried out on chloroprene rubber cylindrical samples under compressive loading to study the load-deflection characteristics of rubber pad. Dimensions of the developed rubber specimen are ϕ 29×12 mm [36]. The compression test specimen shown in Figure 8 is manufactured by molding process. The Universal Testing Machine (Instron 3365) is used for the compression test. The gradual compressive load is applied on the specimen up to a maximum load of 353.44 kgf. After compression test the diameter of the specimen increases by 0.5 mm and height decreases by 0.25 mm approximately. The output data is stored in the computer and the same is represented by graphical form in Figure 9 which indicates the non-linear behavior of developed rubber. The compression test results are given in Table 1.

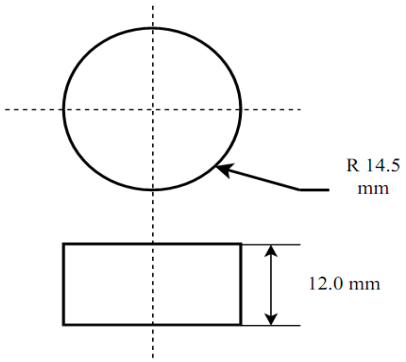

Figure 8. Compression test specimen

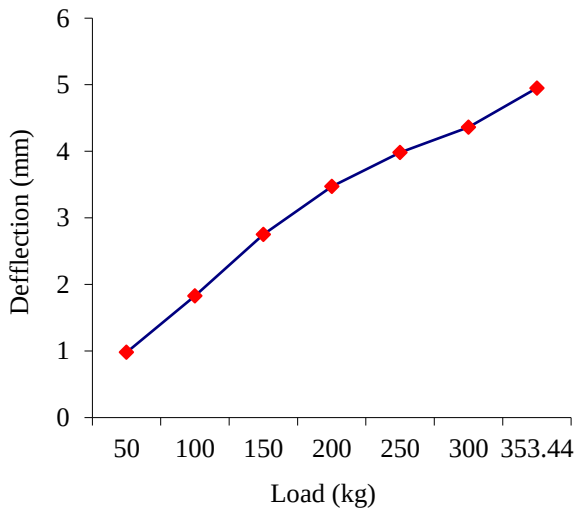

Figure 9. Variation of experimental load and deflection characteristic

Table 1. Experimental compression test results

Sr. No.	Load (in kgf)	Deflection (in mm)
1	50	0.98
2	100	1.83
3	150	2.75
4	200	3.47
5	250	3.98
6	300	4.36
7	353.44 (Max.)	4.95

It is evident that the general curve shape of rubber material differs from that of a metallic material. For this type of material, Young's Modulus is not a significant property because there is no clear linear relationship. To understand how a rubber material will respond to a specific compressive load, one needs consult a CFD curve. Unlike metals, strains cannot be predicted using a straightforward linear connection. The compression test results are used to compare the deflections of anti-vibration pad calculated by using ANSYS software. Both the results show the non-linear load – deflection curves. The deflections observed in the compression test at different compressive loads are within the limit for the developed chloroprene rubber [20]. The compression test is useful to decide whether the developed rubber falls within the expected compression deflection range.

4. FEA OF AN ANTI-VIBRATION MOUNT

Under Indian Railways track conditions, the elastomeric pad positioned between the side frame and adapter experiences compressive and shear loads generated in freight bogies installed in wagons with axle loads of up to 25 tons. Half of the axle load—that is, the load on the wheel sets—is experienced by the EM pad when the vehicle is stationary. This force is amplified under the dynamic situations. The main purpose of the elastomeric pad is to lessen wheel wear. It also serves as an anti-vibration component and improves the steering capability of a three-piece freight stock bogie. In this work the deflection characteristics of anti-vibration mount under compressive loads are studied. Two rubber pads made of chloroprene and three plates of mild steel divide an elastomeric pad. These various materials are thought to be completely linked to one another. Plane 182 element with four nodes is chosen for the model. Solid structure 2-D modeling is done with PLANE182 element. The element can be utilized as an axisymmetric element or as a plane element (plane stress, plane strain, or generalized plane strain). Four nodes, each with two degrees of freedom—translations in the nodal x and y directions—define it. The element can withstand large deflection, large strain, stress stiffening, plasticity, and hyperelasticity. Additionally, it can simulate the deformations of fully incompressible hyperelastic materials and virtually incompressible elastoplastic materials using mixed formulation capabilities. The study used the nonlinear Mooney-Rivlin model with three parameters for hyperelastic materials [36]. ANSYS software analyzes anti-vibration mount model that is depicted in Figure 10. The deformation shape and resultant deflection contour is shown in Figure 11. The resultant maximum deflection of the elastomeric pad observed is 6.352 mm for 10-ton compressive load.

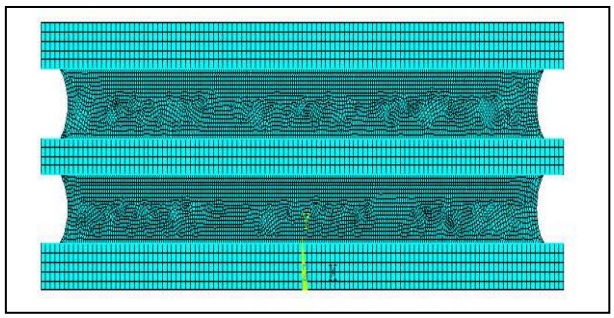

Figure 10. Anti-vibration mount FEA model

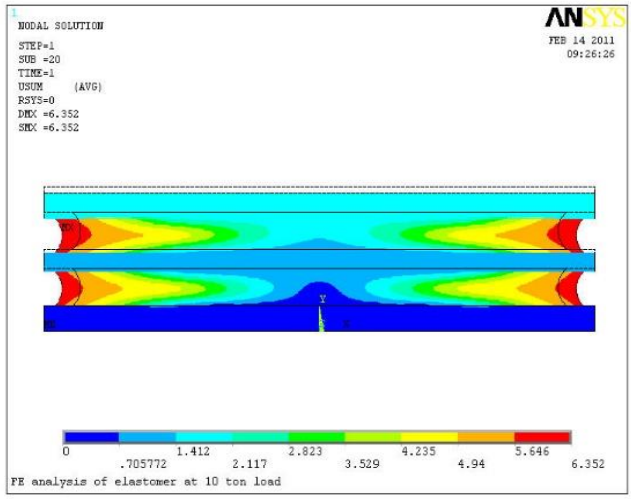

Figure 11. Deformation FEA results for 10-ton compressive load

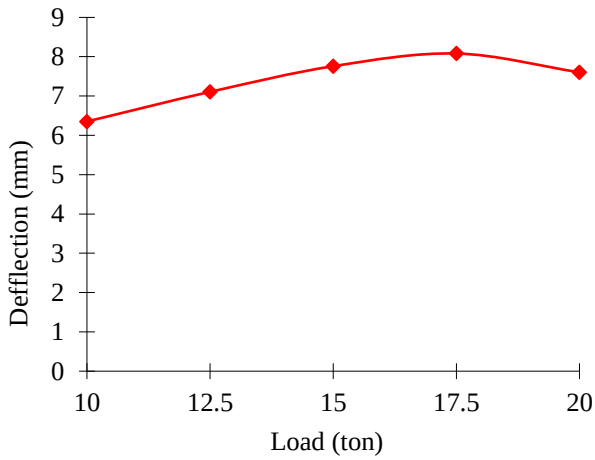

Figure 12. Load deflection characteristic of the pad by FEA

Table 2. Predicted maximum deflection of an anti-vibration mount

Load Ton	10	12.5	15	17.5	20
Max. Deflection in mm	6.35	7.10	7.75	8.08	7.60

The load deflection characteristic of the chloroprene rubber pad by FEA is shown in Figure 12 and experimental load deflection characteristic is shown in Figure 9. From these results it is pointed out that the deflection increases as the load on the pad increases to a certain value and then decreases. From experimental results as well as FEA results, the non-linear load deflection characteristic of developed rubber is observed.

The non-linear behavior of developed chloroprene rubber is observed from the experimental and FEA results. Table 2 shows predicted maximum deflection at different compressive loads. The predicted maximum deflection observed is 8.081 mm at 17.5 tone compressive load. It is observed that the difference between the predicted deflections by FEA and compression test results is below 15% which validates the FEA model. This difference between the experimental and FEA results is observed because only three parameter Moony-Rivlin FEA model is only considered. As we increase the number of parameters in Mooney-Rivlin model then the

accuracy of the model will increase but the computation time required for FEA will increase. The difference between the FEA results and the experimental results will be also minimized by improving the physical properties and geometry accuracy of developed rubber specimens. The predicted load deflection characteristic of chloroprene rubber shows the non-linear behavior. The maximum deflection decides whether the developed rubber sustain for the required period or not. The predicted maximum deflection also decides the required stiffness of the anti-vibration mount. Thus, the predicted maximum deflection, non-linear behavior of chloroprene rubber, and rubber stiffness are useful parameters for design of the anti-vibration mount at an early stage.

5. CONCLUSIONS

To ensure safety and reliability, a methodology is developed to predict the maximum deflection of an anti-vibration mount using an integration of material property tests and analysis by finite element modeling in primary design process. Maximum deflection of the mount must be predicted before the prototype or actual component is created since rubber made of chloroprene material is a recently designed material for an anti-vibration mount to match stated nominal standards. The maximum deflection is seen to increase till a specific limit and decrease afterwards as compressive force on an anti-vibration mount increase, demonstrating the non-linearity of the rubber material. The rubber filler's mechanical response was very different from the rubber matrix's, which could be one reason for this. Because of this, the filler network did not deform as quickly as its rubber matrix counterpart. Rubber typically displays considerable nonlinear behavior when subjected to mechanical loads because of both geometrical and material nonlinearities.

Predicted maximum deflection of an anti-vibration mount in the given load range is 8.081mm. This satisfies the maximum deflection requirement of the Research Development and Standards Organizations (RDSO) of Indian Railway which mentioned the limit of the maximum deflection in the given load range as 10 mm. The difference between the experimental compression test on the developed rubber samples and the results obtained by FEA model is below 15 % which validates the established methodology. The predicted deflection and experimental characteristics match with the results available in the literature [20]. Three more problems make structural analysis of such material using the finite element approach more difficult: In the process of deformation analysis, (1) improper element formulation may result in the locking phenomena, which could lead to incorrect conclusions; (2) polynomial-form constitutive equations may produce material instability; and (3) the usage of low order elements may cause pressure instability. The methodology developed in this study is useful to predict the deflection of any anti-vibration mount with material and geometry which will be helpful at early design stage. The future work of this study is to perform the experimentation on the actual anti-vibration developed and compare the deflection results with the FEA model. In this study the deflections are not calculated by testing anti-vibration mount as it is in the early design stage. The accuracy of the FEA model can be increased by increasing the number of parameters in the Mooney- Rivlin model with high computation facilities which will also increase the overall cost of the work.

ACKNOWLEDGMENT

The authors are thankful to Indian Rubber Manufacturer's Research Association, Thane (W), Maharashtra, India and the Management, Principal Dr. R. V. Patil of Pune District Education Association's College of Engineering, Manjari Bk, Pune, India for supporting this research work.

REFERENCES

[1] Gent, A.N. (2012). Engineering with Rubber. Hanser Gardner Publications, Ohio, USA.

[2] Brown R.P. (2006). Physical Testing of Rubbers. Springer. https://link.springer.com/book/10.1007/0-387-29012-5.

[3] Morton, M. (2013). Rubber Technology. Van Nostrand Reinhold, New York.

[4] Yeoh, O.H. (1997). On the Ogden strain-energy function. Rubber Chemistry and Technology, 70(2): 175-182. https://doi.org/10.5254/1.3538422

[5] Li, Q., Zhao, J.C., Zhao, B. (2009). Fatigue life prediction of a rubber mount based on test of material properties and finite element analysis. Engineering Failure Analysis, 16(7): 2304-2310. https://doi.org/10.1016/j.engfailanal.2009.03.008

[6] Ali, A., Hosseini, M., Sahari, B. (2010). Continuum damage mechanics modeling for fatigue life of elastomeric materials. International Journal of Structural Integrity, 1(1): 63-72. https://doi.org/10.1108/17579861011023801

[7] Mars, W.V., Fatemi, A. (2004). Factors that affect the fatigue life of rubber: A literature survey. Rubber Chemistry and Technology, 77(3): 391-412. https://doi.org/10.5254/1.3547831

[8] Boyce, M.C., Arruda, E.M. (2000). Constitutive models of rubber elasticity: A review. Rubber Chemistry and Technology, 73(3): 504-523. https://doi.org/10.5254/1.3547602

[9] Kim, W.D., Lee, H.J., Kim, J.Y., Koh, S.K. (2004). Fatigue life estimation of an engine rubber mount. International Journal of Fatigue, 26(5): 553-560. https://doi.org/10.1016/j.ijfatigue.2003.08.025

[10] Lake, G.J. (1995). Fatigue and fracture of elastomers. Rubber Chemistry and Technology, 68(3): 435-460. https://doi.org/10.5254/1.3538750

[11] Morman Jr, K.N., Pan, T.Y. (1988). Application of finite-element analysis in the design of automotive elastomeric components. Rubber Chemistry and Technology, 61(3): 503-533. https://doi.org/10.5254/1.3536198

[12] Oh, H.L. (1980). A fatigue-life model of a rubber bushing; Rubber Chemistry and Technology, 53: 1226-1238. https://doi.org/10.5254/1.3535090

[13] Hirakawa, H., Urano, F., Kida, M. (1978). Analysis of fatigue process of rubber vulcanizates. Rubber Chemistry and Technology, 51(2): 201-214. https://doi.org/10.5254/1.3545829

[14] Mullins, L. (1969). Softening of rubber by deformation. Rubber Chemistry and Technology, 42(1): 339-362. https://doi.org/10.5254/1.3539210

[15] Marckmann, G., Verron, E. (2006). Comparison of hyperelastic models for rubber-like materials. Rubber Chemistry and Technology, 79(5): 835-858. https://doi.org/10.5254/1.3547969

[16] Cadwell, S.M., Merrill, R.A., Sloman, C.M., Yost, F.L. (1940). Dynamic fatigue life of rubber. Rubber Chemistry and Technology, 13(2): 304-315. https://doi.org/10.5254/1.3539515
[17] Saintier, N., Cailletaud, G., Piques, R. (2006). Multiaxial fatigue life prediction for a natural rubber. International Journal of Fatigue, 28(5-6): 530-539. https://doi.org/10.1016/j.ijfatigue.2005.05.011
[18] Le Cam, J.B., Huneau, B., Verron, E., Gornet, L. (2004). Mechanism of fatigue crack growth in carbon black filled natural rubber. Macromolecules, 37(13): 5011-5017. https://doi.org/10.1021/ma0495386
[19] Lindley, P.B. (1973). Relation between hysteresis and the dynamic crack growth resistance of natural rubber. International Journal of Fracture, 9: 449-462. https://doi.org/10.1007/BF00036325
[20] Mars, W.V., Fatemi, A. (2002). A literature survey on fatigue analysis approaches for rubber. International Journal of Fatigue, 24(9): 949-961. https://doi.org/10.1016/S0142-1123(02)00008-7
[21] Saintier, N., Cailletaud, G., Piques, R. (2006). Crack initiation and propagation under multiaxial fatigue in a natural rubber. International Journal of Fatigue, 28(1): 61-72. https://doi.org/10.1016/j.ijfatigue.2005.03.006
[22] Kim, J.H., Jeong, H.Y. (2005). A study on the material properties and fatigue life of natural rubber with different carbon blacks. International Journal of Fatigue, 27(3): 263-272. https://doi.org/10.1016/j.ijfatigue.2004.07.002
[23] Mars, W.V., Fatemi, A. (2005). Multiaxial fatigue of rubber: Part I: Equivalence criteria and theoretical aspects. Fatigue & Fracture of Engineering Materials & Structures, 28(6): 515-522. https://doi.org/10.1111/j.1460-2695.2005.00891.x
[24] Legorju-Jago, K., Bathias, C. (2002). Fatigue initiation and propagation in natural and synthetic rubbers. International Journal of Fatigue, 24(2-4): 85-92. https://doi.org/10.1016/S0142-1123(01)00062-7
[25] Luo, R.K., Wu, W.X. (2006). Fatigue failure analysis of anti-vibration rubber spring. Engineering Failure Analysis, 13(1): 110-116. https://doi.org/10.1016/j.engfailanal.2004.10.012
[26] Le Cam, J.B., Huneau, B., Verron, E. (2008). Description of fatigue damage in carbon black filled natural rubber. Fatigue & Fracture of Engineering Materials & Structures, 31(12): 1031-1038. https://doi.org/10.1111/j.1460-2695.2008.01293.x
[27] Verron, E., Andriyana, A. (2008). Definition of a new predictor for multiaxial fatigue crack nucleation in rubber. Journal of the Mechanics and Physics of Solids, 56(2): 417-443. https://doi.org/10.1016/j.jmps.2007.05.019
[28] Ali, A., Hosseini, M., Sahari, B.B. (2010). A review of constitutive models for rubber-like materials. American Journal of Engineering and Applied Sciences, 3(1): 232-239.
[29] Mars, W.V., Fatemi, A. (2006). Multiaxial stress effects on fatigue behavior of filled natural rubber. International Journal of Fatigue, 28(5-6): 521-529. https://doi.org/10.1016/j.ijfatigue.2005.07.040
[30] Woo, C.S., Kim, W.D. (2006). Heat-aging effects on the material properties and fatigue life prediction of vulcanized natural rubber. e-Journal of Soft Materials, 2: 7-12. https://doi.org/10.2324/ejsm.2.7
[31] Andriyana, A., Verron, E. (2007). Prediction of fatigue life improvement in natural rubber using configurational stress. International Journal of Solids and Structures, 44(7-8): 2079-2092. https://doi.org/10.1016/j.ijsolstr.2006.06.046
[32] Stevenson, A., Hawkes, J.R., Harris, J.A., Hansen, P. (1998). Fatigue life of elastomeric engineering components under biaxial loading using finite element analysis (No. 982310). SAE Technical Paper. https://doi.org/10.4271/982310
[33] Lewitzke, C., Lee, P. (2001). Application of elastomeric components for noise and vibration isolation in the automotive industry (No. 2001-01-1447). SAE Technical Paper. https://doi.org/10.4271/2001-01-1447
[34] Martin, J.M., Smith, W.K. (2019). Handbook of Rubber Technology. CBS Publication, New Delhi, pp. 301-311. https://eduport-global.com/product/handbook-rubber-technology-vol-2.
[35] Rivlin, R.S., Sawyers, K.N. (1976). The strain-energy function for elastomers. Transactions of the Society of Rheology, 20(4): 545-557. https://doi.org/10.1122/1.549436
[36] ASTM Standards. (1984). ASTM Volume 09.02: Rubber Products, Industrial — Specifications and Related Test Methods, Gaskets, Tires. https://www.astm.org/astm-bos-09.02.html.

NOMENCLATURE

$\boldsymbol{M}$	mass, Kg
K	stiffness, N/mm
F	force, N
f	frequency, Hz
t	time, sec
Y	displacement, mm
T	transmissibility
C	constant
E	modulus of elasticity, N/mm^2
I	strain invariant
W	strain energy potential

Greek symbols

ω	angular frequency of vibration, cycle/sec
Δ	deflection, mm
δ	deformation, mm
ξ	damping ratio
υ	Poison's ratio
$_\infty$	infinity
λ	stretch ratio

Subscripts

$_o$	initial
$_n$	natural
$_s$	static
$_{ijk}$	vector directions